Induced circular dichroism spectra of α-, β-, and γ-cyclodextrin complexes with π-conjugate compounds. Part 2. Chiral dimer formation and polarization directions of the π–π* transitions in some hydroxyazo guests having a naphthalene nucleus †

Noboru Yoshida,*[a] Hiroyuki Yamaguchi,[b] Tomoaki Iwao[b] and Miwako Higashi[c]

[a] *Laboratory of Molecular Functional Chemistry, Division of Material Science, Graduate School of Environmental Earth Science, Hokkaido University, Sapporo 060, Japan*
[b] *Faculty of Engineering, Department of Materials Science, Ibaraki University, Hitachi 316, Japan*
[c] *Center for Cooperative Research and Development, Ibaraki University, Hitachi 316, Japan*

Received (in Cambridge) 18th May 1998, Accepted 25th November 1998

The absorption and circular dichroism spectra of some *o*- and *p*-hydroxyazo compounds having a naphthalene nucleus in the presence of α-, β-, and γ-cyclodextrin (CDx) have been measured in the wavelength region of 200–600 nm. The induced circular dichroism (ICD) is observed on the absorption bands of the π–π* transitions of the azo chromophore and the naphthalene moiety. The signs in the observed ICD spectra are discussed in terms of the orientation of the transition moment of the π–π* states to the axis of the CDx cavity and the polarization analysis by using the ZINDO approximation. Judging from the single positive sign of the ICD signal, the polarization directions of the first π–π* transitions of the azo chromophore are almost parallel to the CDx axis. Some β- and γ-CDx complexes of the title azo compounds show a split-type [(+) to (−) or (−) to (+)] ICD band at the π–π* transitions of the azo group, suggesting that a chiral dimer is trapped within the CDx cavity. The ICD bands of the naphthalene moiety may also be useful to detect the formation of the chiral dimer.

Introduction

The analysis of the ICD spectral pattern of the chromophore of aromatic compounds in the presence of CDx has been given much attention in the past decade as a suitable technique for spectral band assignments of the electronic transitions[1] and elucidation of the inclusion complexes where their chromophores are situated inside the CDx cavity.[2]

Harata and Uedaira[1l] have measured the ICD spectra of β-CDx complexes with some naphthalene derivatives and estimated the orientation of the chromophore within the β-CDx cavity on the basis of the Kirkwood–Tinoco equation. Yamaguchi *et al.* have shown that the symmetry species of the vibrational modes can be identified from the signs of the β-CDx complexes with fluorobenzene, bromobenzene, toluene, and benzonitrile.[1f] The direction of the electronic transition moment in the β-CDx cavity of 2-hydroxytropone,[1i] azulene,[1j] substituted benzenes,[1h] azanaphthalenes,[1d] and nitrogen heterocycles[1a] has been discussed in terms of the sign and intensity of ICD spectra of their CDx inclusion complexes.

On the other hand, ICD provides precise structural information such as the orientation of the chromophore in the CDx cavity. The strong split-type ICD spectra like an exciton coupling effect have been observed frequently and this typical spectral change suggests the formation of a 2:2 (CDx:guest) inclusion complex where a chiral dye dimer is trapped within the CDx cavity (Scheme 1).[1b,2c,g–i] Thus, the chromophore in dyes such as azo compounds[3] and cyanines[4] has been used as the most useful ICD probe for the detection of chiral environment.

Although our kinetic[5] and equilibrium[6] studies of the molecular recognition between the anionic azo compounds and CDx have provided useful information concerning the rate, mechanism, and direction for inclusion, precise structural information such as the orientation of the chromophore in the CDx cavity could be obtained from the analysis of the ICD spectral pattern of the inclusion complexes. Changes in the relative intensities and spectral patterns of circular dichroism bands reflect the asymmetric interactions of the CDx:guest complexes. Our recent studies on the cyclodextrin-induced asymmetry of various achiral azo compounds suggest that the ICD spectral patterns are largely dependent on the position and number of alkyl-substituents of the azo guest molecules.[2c]

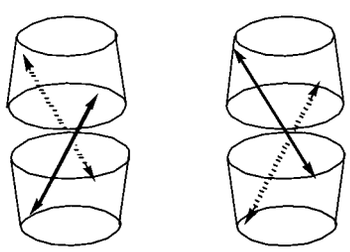

Scheme 1

In our previous work, we have studied the ICD spectra of α-, β-, and γ-CDx inclusion complexes with **1** and **2** in aqueous

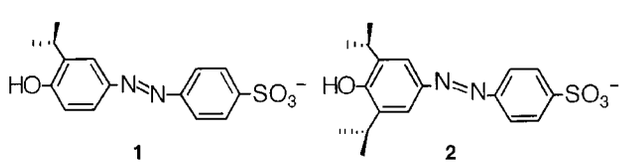

1 **2**

solution and revealed that the sign and intensity of ICD spectra depend on the direction of the transition moment of the azo chromophore with respect to the CDx axis.[2c] Furthermore, negative (−) split-type ICD spectra have been observed particu-

† For Part 1, see ref. 2(*c*).

larly in the π–π* transition band of the –N=N– group of the **2**–*β*CDx and **2**–*γ*CDx inclusion complexes, suggesting the formation of (−) chiral dimer in the CDx cavity (Scheme 1).

In general, the ICD pattern of the host–guest complexes which is closely related to the stability of the inclusion complexes, the cavity size of CDx, the position and orientation of the chromophore in the CDx cavity, and the subtle change in the structure of the guest may be rationalised after the event but can rarely be predicted in advance. Here, we report various ICD spectral patterns in the *α*-, *β*-, and *γ*-CDx inclusion complexes with *o*- and *p*-hydroxyazo compounds **3**–**8** having a naphthalene nucleus.

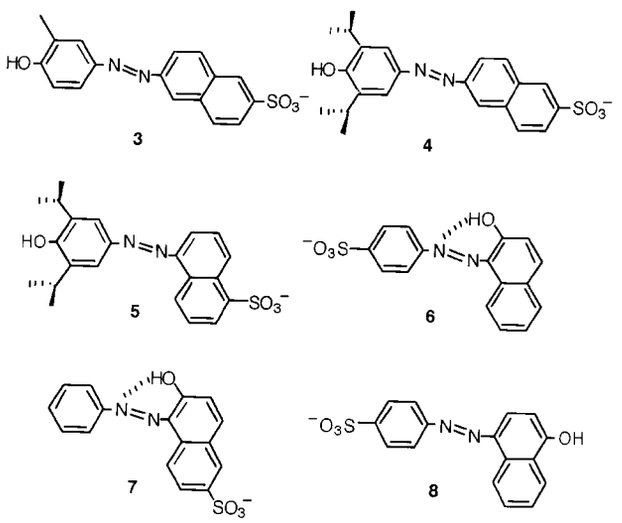

A comparison of the ICD pattern of the azo chromophore with that of the naphthalene moiety would also be helpful for elucidation of the detailed solution structure of the CDx inclusion complexes.

Experimental

Materials

The azo guest molecules **3**–**5** were synthesized and purified.[7,8] The azo dyes **6**–**8** were purchased from Fluka. Cyclodextrins were obtained from Tokyo Kasei Kogyo Co. and used as received. All other materials were commercially available and used without purification unless otherwise stated.

Measurements

The pH in solution was obtained using a Horiba pH meter D-13. The temperature was maintained at 25 °C by means of an external circulating water bath. The absorption spectra were obtained with Hitachi U-3200 and JASCO V-550 spectrophotometers. The CD spectra were measured using a JASCO J-600C circular dichrometer. In order to obtain an adequate signal-to-noise ratio, we used a computer for multiple scanning and averaging. Each memory unit in the computer stored the CD signal for a spectral band of 0.2 nm. All other conditions are the same as described previously.[2c]

Results and discussion

Absorption and induced CD spectra of the cyclodextrin inclusion complexes of 3–5

Aqueous solutions of **3**–**5** exhibit a colour change from yellow to orange with increasing pH in solution. This is due to the deprotonation of the *p*-hydroxy group of **3**–**5** (HA^-, pK_a = 8.0–8.5).[5b] Therefore, the ICD spectra were obtained at pH 4 where the dye anion, HA^-, is present.

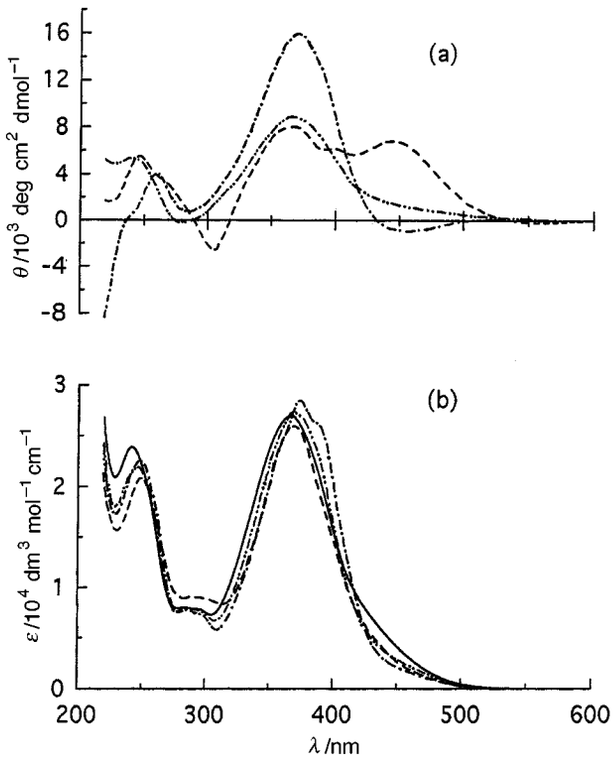

Fig. 1 Induced circular dichroism (a) and absorption (b) spectra of the *α*- (·····), *β*- (·····), and *γ*-cyclodextrin (----) complexes of **3** at pH 4 and 25 °C. [**3**] = 6.61×10^{-5} mol dm^{-3} and [cyclodextrins] = 1.2×10^{-2} mol dm^{-3}. Guest only (solid line).

Fig. 1 shows the CD (upper) and UV–vis (lower) spectra of *α*-, *β*-, *γ*-CDx complexes with **3** in aqueous solution. Transition energies and moments of **3**–**5** were calculated by the ZINDO method[9] and are given in Table 1. On the assumption that these compounds are almost planar, the geometries were optimized by using the PM3 method.[10] A large positive ICD enhancement in the first π–π* band of –N=N– of **3** at 366 nm which is assigned to the long-axis polarized transition [bands (2) and (3) in Scheme 2] is observed in all CDx complexes. Harata's rule

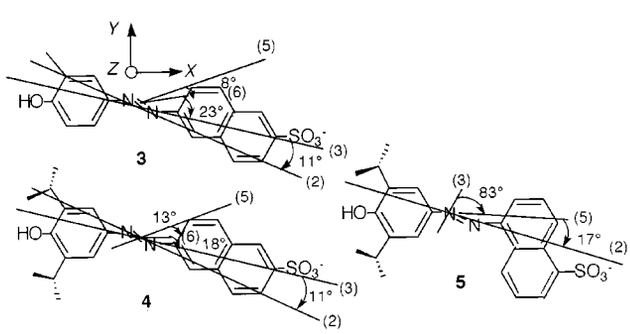

Scheme 2

suggests that the polarization of this transition is almost parallel to the symmetry axis of the CDx cavity. Typical ICD patterns such as a strong positive at the π–π* band and a very weak negative at the n–π* band of the –N=N– group are observed only in *α*-CDx. The relatively strong positive (*γ*-CDx), weak positive (*β*-CDx), and weak negative (*α*-CDx) ICD signs at *ca.* 450(sh) nm assigned to an n–π* transition of –N=N– (forbidden band 1 in Table 1) of **3** depend also on the direction of the chromophore to the CDx axis.[2c] Although effects due to the conformational changes or minor structural changes such as the different torsions of the respective chromophores should be considered, a reasonable explanation of the ICD intensity at n–π* is not clear at the present stage. The weaker ICD band at

Table 1 Experimental transition and extinction coefficients (ε/dm^3 mol^{-1} cm^{-1}) and calculated results of transition energies (λ_{max}/nm) and oscillator strengths (f) of **3**, **4** and **5** by the ZINDO method

		Experimental		Calculation		
Compound	Band	λ_{max}	ε	λ_{max}	f	Polarization[a]
3	1			525	0.00	n–π*(–N=N–)[b]
	2	366	27100	349	0.610	28 π–π*(–N=N–)[c]
	3			323	0.560	17 π–π*(–N=N–)[d]
	4			292	0.004	53
	5	~240	24000	277	0.489	−14 π–π*(Naph)[e]
	6			263	0.036	−6 π–π*(Naph)[f]
	7			244	0.007	
4	1			500	0.000	n–π*(–N=N–)
	2	369	18200	348	0.610	28 π–π*(–N=N–)
	3			321	0.570	17 π–π*(–N=N–)
	4			301	0.001	−33
	5	~240	17500	277	0.469	−14 π–π*(Naph)
	6			261	0.027	−1 π–π*(Naph)
	7			246	0.020	
5	1			516	0.000	n–π*(–N=N–)
	2	375	16100	366	0.781	17 π–π*(–N=N–)
	3			317	0.003	−80 π–π*(Naph)
	4			302	0.000	−33
	5	~250 (sh)		270	0.126	3 π–π*(Naph)
	6	~230 (sh)		261	0.264	
	7			258	0.159	
	8			233	0.206	

[a] The angle of the transition moment to the x-axis. [b] $-0.884\varphi(55\rightarrow62) - 0.366\varphi(55\rightarrow66)$ where φ_{55}, φ_{62}, and φ_{66} are the n orbital of –N=N–, the π orbital of –N=N–, and the φ_{B2g} of naphthalene, respectively. [c] The charge transfer from naphthalene to –N=N–. $0.885\varphi(61\rightarrow62)$ where φ_{61} is the φ_{Au} of naphthalene and φ_{62} the π orbital of –N=N–. [d] The charge transfer from naphthalene to –N=N–. $0.760\varphi(60\rightarrow62) - 0.304\varphi(60\rightarrow64)$ where φ_{60} is the φ_{B1u} of napththalene and φ_{64} the φ_{B3g} of napththalene. [e] $-0.613\varphi(61\rightarrow64) + 0.465\varphi(60\rightarrow62) + 0.369\varphi(58\rightarrow62) + 0.388\varphi(61\rightarrow65)$. [f] $0.464\varphi(61\rightarrow64) + 0.461\varphi(60\rightarrow64) + 0.441\varphi(61\rightarrow66) + 0.311\varphi(60\rightarrow62)$.

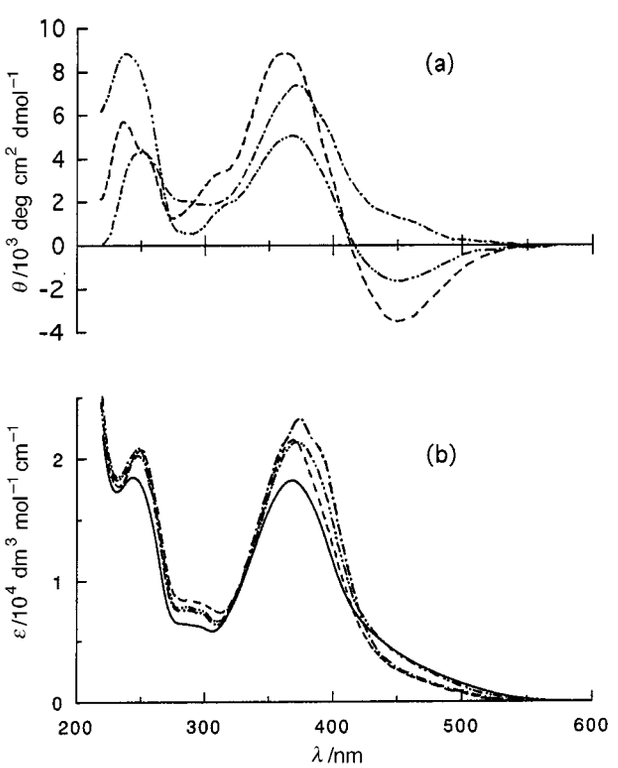

Fig. 2 Induced circular dichroism (a) and absorption (b) spectra of the α- (·····), β- (·····), and γ-cyclodextrin (----) complexes of **4** at pH 4 and 25 °C. [**4**] = 7.50×10^{-5} mol dm^{-3} and [cyclodextrins] = 1.2×10^{-2} mol dm^{-3}. Guest only (solid line).

the π–π* transition moment of the naphthalene group [*ca.* 250 nm in Fig. 1 and bands (5) and (6) in Scheme 2] indicates that the angle of this transition is smaller to the CDx axis.

Fig. 2 shows the CD (upper) and UV–vis (lower) spectra of α-, β-, γ-CDx complexes with **4**.

Since α-CDx does not bind from the 3′,5′-diisopropylphenol side of **4** owing to the larger steric hindrance,[5b] only inclusion from the naphthalenesulfonate side could be anticipated. It is noteworthy that the ICD spectra of **4**–α**CDx** have strong positives at the π–π* band of –N=N– and the naphthalene nucleus. The structures of α-, β-, and γ-CDx complexes with **4** are quite similar to each other as judged by the analogous ICD patterns in Fig. 2 except for the n-π* band.

The structural difference between **4** and **5** is the α- and β-positions of the 3,5-$(Pr^i)_2$(4-OH)C_6H_2–N=N– group attached to the naphthalene side. Fig. 3 shows the CD (upper) and UV–vis (lower) spectra of α-, β-, and γ-CDx complexes with **5**.

Because of the full block[5b] from both sides of phenol and naphthalene [β-position of 3,5-$(Pr^i)_2$(4-OH)C_6H_2–N=N– group], the ICD signal of **5**–α**CDx** is very weak compared with that of **3**–α**CDx** and **4**–α**CDx**. In contrast to the **5**–β**CDx** and **5**–γ**CDx** complexes, the ICD spectrum of the **5**–α**CDx** complex is very weak in all wavelength regions as mentioned above. Such a subtle modification in structure between **4** and **5** causes a drastic change in the ICD spectral pattern in Fig. 2 and 3. Furthermore, high-intensity spectra with symmetric negative (+/−) split-type signals which are very similar to those of **2**–β**CDx** and **2**–γ**CDx**[2c] are observed in **5**–β**CDx** and **5**–γ**CDx** complexes, indicating that the chiral dimers, (**5**–β**CDx**)$_2$ and (**5**–γ**CDx**)$_2$, are formed (Scheme 1). UV–vis titration data also support the formation of these dimers. In general, a split-type ICD pattern appears to originate with a dipole–dipole interaction between the electric transition moments of the two chromophores. The representative split-type ICD has been applied to many twisted π-electron systems as the CD exciton chirality method.[11] A weaker but analogous split-type ICD pattern is observed in the UV region (200–250 nm) of **5**–β**CDx** and **5**–γ**CDx**. The two main bands at 200–250 nm and at 375 nm could be assigned to the nearly short and long-axis

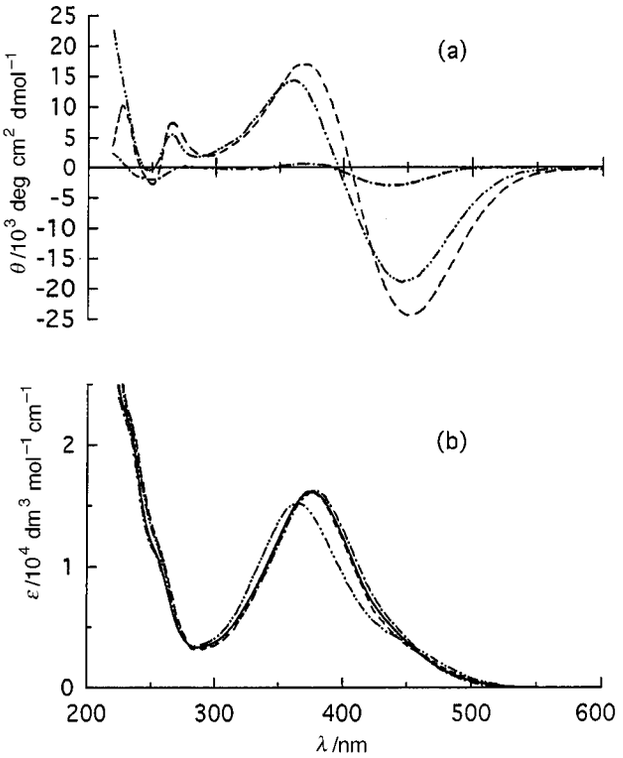

Fig. 3 Induced circular dichroism (a) and absorption (b) spectra of the *α*- (·····), *β*- (·····), and *γ*-cyclodextrin (----) complexes of **5** at pH 4 and 25 °C. [**5**] = 4.98×10^{-5} mol dm^{-3} and [cyclodextrins] = 1.2×10^{-2} mol dm^{-3}. Guest only (solid line).

polarized π–π* transition of the naphthalene moiety and the long-axis polarized π–π* transition of the –N=N– group of **5**, respectively (Table 1 and bands (2) and (5) in Scheme 2).

Absorption spectra of 6–8

The λ_{max} at the longest visible band in the region of 440–550 nm, which is probably attributable to the π–π* transition of the –N=N– group of **6**–**8**, is more shifted to longer wavelength compared with the λ_{max} in the region of 300–500 nm of **3**–**4**. Since the azo compounds **6** and **7** have the higher pK_a (=11–12) values and show very slow rate constants (6.9×10^5 dm^3 mol^{-1} s^{-1}) for deprotonation with OH^- ion, there would be –OH · · · N intramolecular hydrogen bonding.[12]

It should be noted that the position and intensity of the first π–π* transition of the –N=N– group are very sensitive to keto-enol tautomerism. A number of spectroscopic studies have established that these types of azo compounds can exist in solution as azo or as hydrazone tautomers.[13] The predominant species of **6** and **8** are probably the hydrazone forms in aqueous

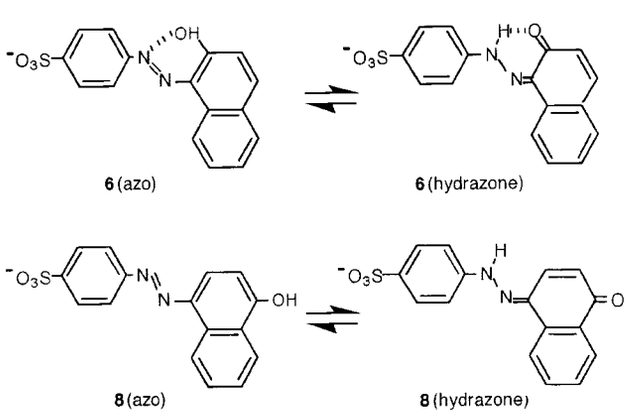

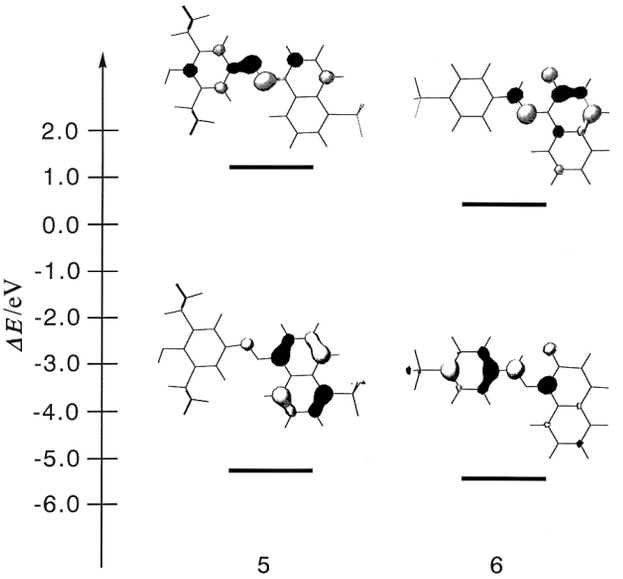

Fig. 4 Energy levels and coefficients of the occupied and vacant orbitals for the first π–π* bands of **5** and **6**.

solution.[2i] The hydrazone form of **8** appears to be also favored by polar solvents and by electron-withdrawing substituents in the phenyl ring.[13]

Therefore, the theoretical spectra calculated as the hydrazone form by the ZINDO method of **6**, **7**, and **8** rather than the azo form agree well with the experimental results (Table 2).

It is noteworthy that the n–π* bands of the –N=N– group are not observed in the UV–vis region. Fig. 4 shows the energy level and coefficient of the occupied and vacant orbitals for the first π–π* bands of **5** and **6**. This energy diagram in Fig. 4 explains the appearance at longer wavelength of the π–π* band of **6**–**8** (475–484 nm) than **3**–**5** (366–375 nm).

The theoretical spectra of **6** and **7** are somewhat different particularly in the π–π* band of the –N=N– group (Table 2), but their experimental absorption spectra are very similar to each other and almost independent of the electronic effects exerted by the position of the $–SO_3–$ group as shown in Fig. 5 and 6. However, the position of the OH group would give a large effect both in the theoretical and experimental spectra as observed in **6** and **8**.

Induced CD spectra of the cyclodextrin inclusion complexes of 6–8

Fig. 5 shows that the first π–π* transitions [band (2) in Scheme 3] of the –N=N– group of **6** gave an unsymmetrical split-type negative (+/−) signal in **6**–*γ*CDx and a positive (−/+) ICD signal in **6**–*β*CDx.

These split-type ICD spectra are characteristic of exciton splitting caused by dimerization of the dye within a chiral environment.[14] Two degenerate transition moments in close proximity and in the appropriate orientation are known to produce high-intensity exciton spectra.[2i] The marked difference in ICD signals with opposite sign between **6**–*β*CDx and **6**–*γ*CDx probably indicates the difference in the dimer geometry within the CDx cavity.

These typical exciton-split bisignate CD bands are also observed in the UV region at the π–π* transition of the naphthalene chromophore. The values of λ_{max} in **6**–*β*CDx (220.6 nm, $\varepsilon = 20800$ dm^3 mol^{-1} cm^{-1}) and **6**-*γ*CDx (230.0 nm, $\varepsilon = 18000$ dm^3 mol^{-1} cm^{-1}) coincide well with the cross points ($\lambda_{cross} = 230.3$ nm for **6**–*β*CDx and 231.3 nm for **6**–*γ*CDx) of their bisignate spectra.

The precise agreement of λ_{max} in the absorption spectrum with λ_{cross} in the ICD spectrum could be predicted by the

Table 2 Experimental transition and extinction coefficients (ε/dm^3 mol^{-1} cm^{-1}) and calculated results of transition energies (λ_{max}/nm) and oscillator strengths (f) calculated as hydrazone forms in **6**, **7**, and **8** by the ZINDO method

		Experimental		Calculation		
Compound	Band	λ_{max}	ε	λ_{max}	f	Polarization[a]
6	1			475	0.000	n(=O)–π*
	2	484	14800	439	0.710	7 π–π*(–N=N–)[b]
	3	310	6370	318	0.149	77
	4	262	8580	307	0.063	57 π–π*(Naph)
	5			296	0.003	63
	6			273	0.216	−63
	7	255	8710	270	0.236	−73 π–π*(Naph)
	8	~236	~22000			π–π*(Naph)
7	1			472	0.000	n(=O)–π*
	2	483	16400	407	0.506	4 π–π*(–N=N–)[c]
	3	317	8080	354	0.288	62 π–π*(–N=N–)[c]
	4	286	6080	299	0.144	27
	5			289	0.026	85
	6	~262	11700	265	0.439	64 π–π*(Naph)
	7			252	0.089	19 π–π*(Naph)
	8	~240	~25000			π–π*(Naph)
8	1	475	29600	415	1.038	15 π–π*(–N=N–)[d]
	2			407	0.000	n(=O)–π*
	3	~326	~6700	301	0.007	4 π–π*(Naph)
	4			288	0.002	−51
	5			285	0.038	43
	6			275	0.160	−61
	7			268	0.165	60
	8			263	0.029	74
	9	287	10700	256	0.233	−5
	10	269	11900	234	0.244	−17
	11			229	0.000	n–π*
	12	240	12200	226	0.123	−90 π–π*(Naph)

[a] The angle of the transition moment to the x-axis. [b] The charge transfer from benzene to –N=N–naphthalene. $-0.997\varphi(58\rightarrow59)$ where φ_{58} is the benzene (φ_{E1g})–N and φ_{59} the π orbital of –N=N–naphthalene. [c] The charge transfer from naphthalene to –N=N–naphthalene. The bands 2 and 3 correspond to $0.980\varphi(58\rightarrow59)$ and $\varphi(57\rightarrow59)$, respectively, where φ_{58}, φ_{57}, and φ_{59} are the π orbital of –N=N–naphthalene, the φ_{B1u} of naphthalene, and the π orbital of –N=N–naphthalene, respectively. [d] The charge transfer from benzene to –N=N–naphthalene. $-0.972\varphi(58\rightarrow59)$.

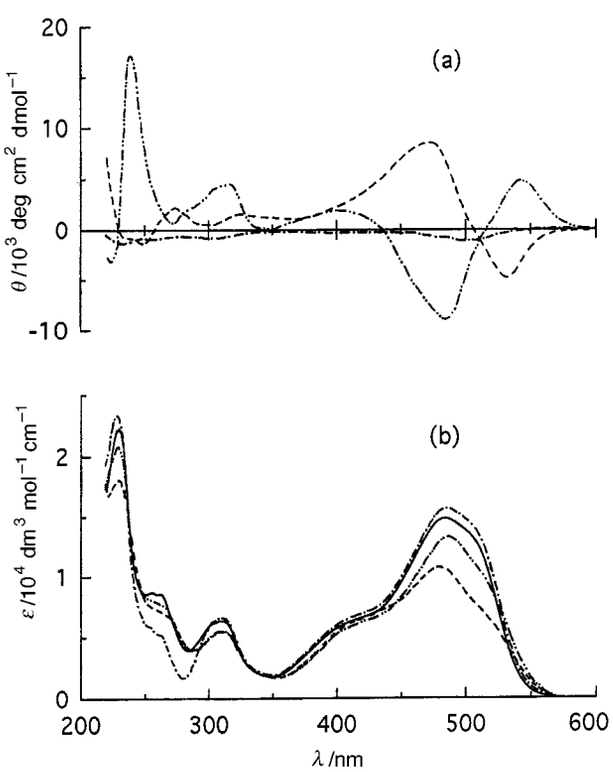

Fig. 5 Induced circular dichroism (a) and absorption (b) spectra of the α- (-·-·-), β- (·····), and γ-cyclodextrin (----) complexes of **6** at pH 4 and 25 °C. [**6**] = 5.46×10^{-5} mol dm^{-3} and [cyclodextrins] = 1.2×10^{-2} mol dm^{-3}. Guest only (solid line).

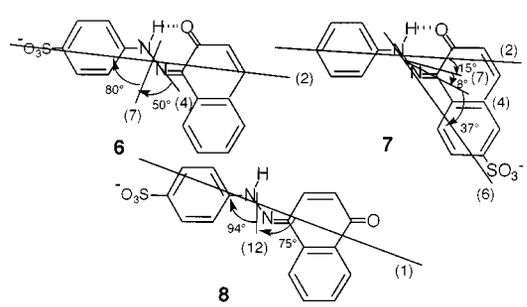

Scheme 3

exciton-coupled theory.[11] However, in the first π–π* transition of the –N=N– group, the crossover point (λ_{cross}) of these ICD spectra is not always coincident with the λ_{max} except for (**8**–βCDx)$_2$. This is often observed and may be due to a less fixed configuration which produces a dipole coupling type ICD. The molar ratio method applied to UV–vis titration data of the **6**–β, γ–CDx systems shows the breaks at [CDx]/[**6**] = 1/2 and 2/2. These breaks have already been observed in the **2**–βCDx system and support the 2:2 stoichiometry.[2c]

A negative (−/+) ICD signal is also observed for the π–π* transition bands of both –N=N– and naphthalene [λ_{max} = 242.0 nm (ε = 20000 dm^3 mol^{-1} cm^{-1}) and λ_{cross} = 242.2 nm] chromophores in **7**–γCDx but it is somewhat weaker as shown in Fig. 6. In **7**–βCDx, the negative split-type ICD is a very obscure one, but the blue shift in λ_{max} and a large hypochromic effect in ε_{max} at the π–π* (–N=N–) transition in Fig. 6 support strongly the formation of the dimer. These observed split-type ICD patterns are closely related to the formation of the chiral 2:2 (host:guest) dimers such as (**6**–βCDx)$_2$, (**6**–γCDx)$_2$, (**7**–γCDx)$_2$,

(**8**–βCDx)$_2$ within a chiral environment. The formation of the chiral dimer may be induced by the stacking of the 1:1 (CDx : guest) inclusion complex.[2c]

The binding with α-CDx produced a slight negative ICD for **6** and **7** at the π–π^* (–N=N–) transition, suggesting the formation of a very unstable complex with a shallower inclusion

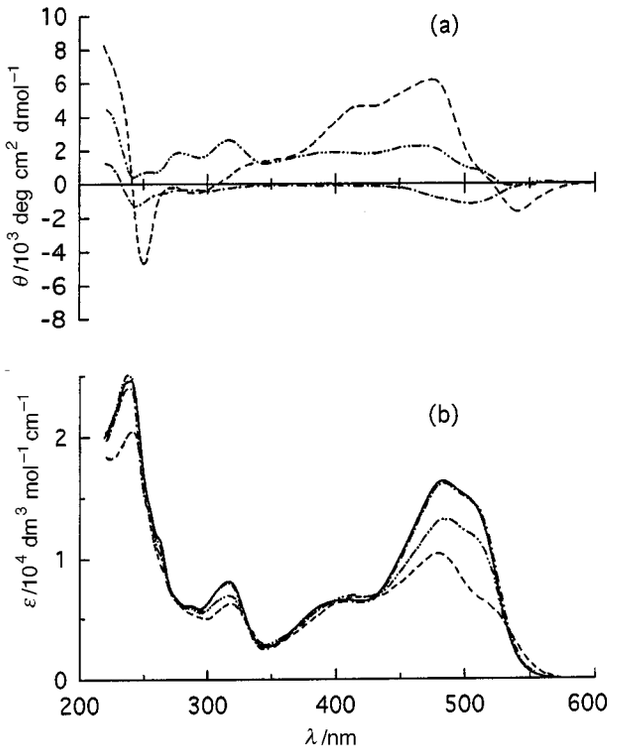

Fig. 6 Induced circular dichroism (a) and absorption (b) spectra of the α- (·····), β- (·····), and γ-cyclodextrin (----) complexes of **7** at pH 4 and 25 °C. [**7**] = 5.73×10^{-5} mol dm^{-3} and [cyclodextrins] = 1.2×10^{-2} mol dm^{-3}. Guest only (solid line).

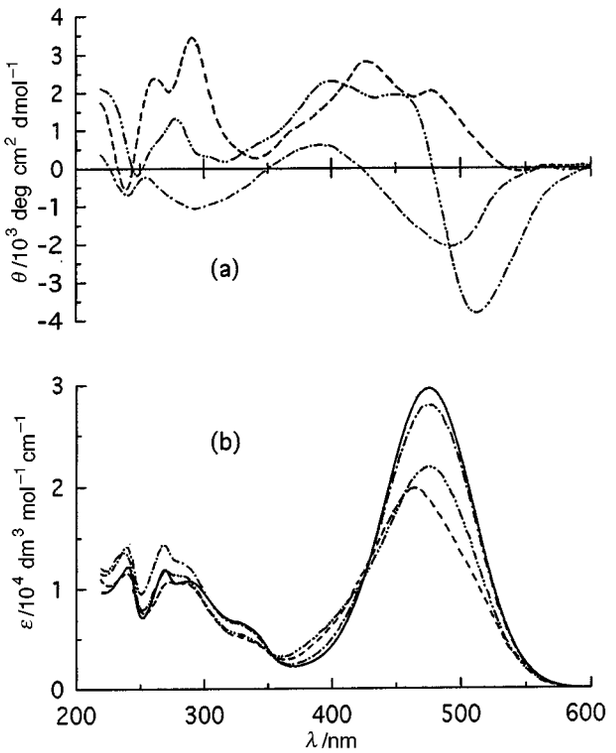

Fig. 7 Induced circular dichroism (a) and absorption (b) spectra of the α- (·····), β- (·····), and γ-cyclodextrin (----) complexes of **8** at pH 4 and 25 °C. [**8**] = 5.00×10^{-5} mol dm^{-3} and [cyclodextrins] = 1.2×10^{-2} mol dm^{-3}. Guest only (solid line).

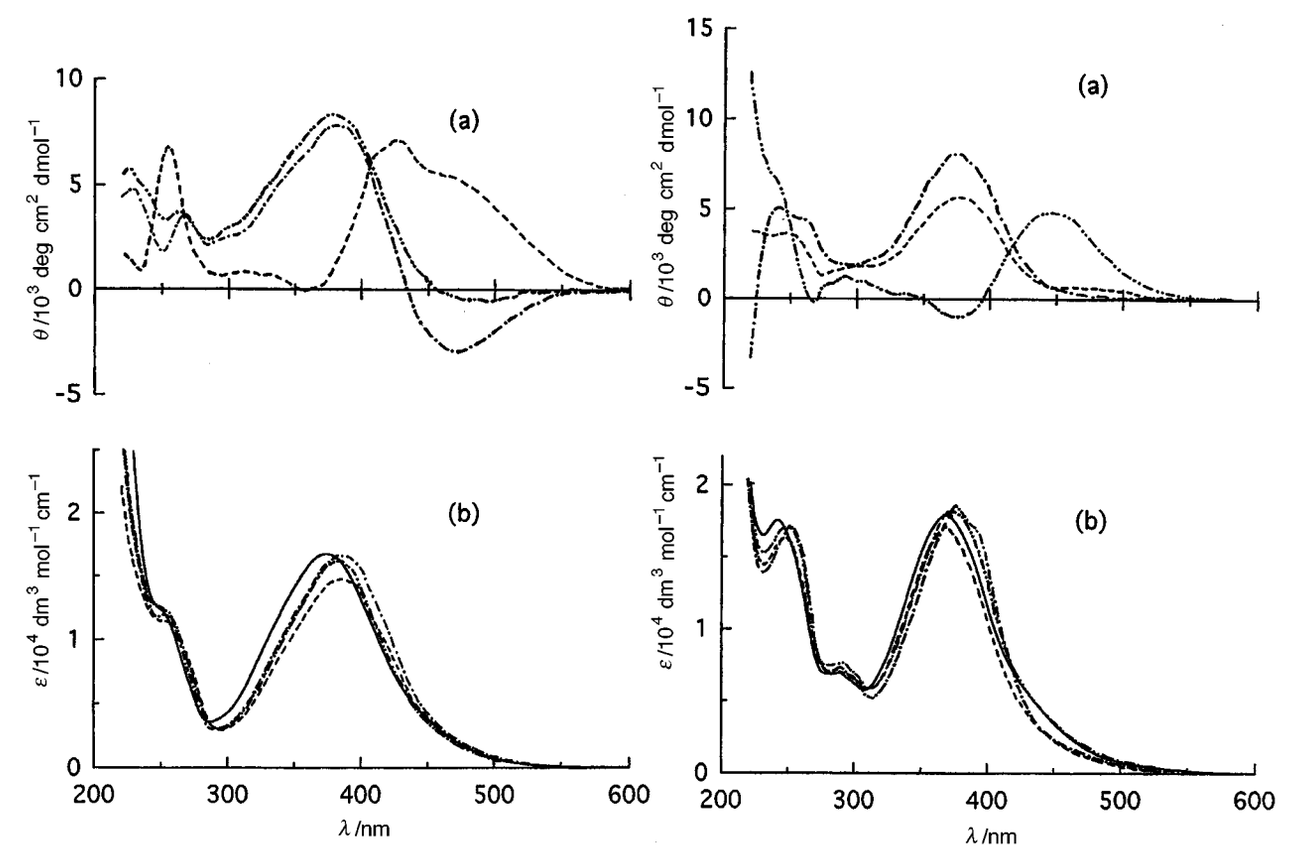

Fig. 8 Induced circular dichroism (a) and absorption (b) spectra of the α- (·····), β- (·····), and γ-cyclodextrin (----) complexes of **9** (left) and **10** (right) at pH 4 and 25 °C. [**9**] = 5.27×10^{-5} mol dm^{-3}, [**10**] = 6.01×10^{-5} mol dm^{-3} and [cyclodextrins] = 1.2×10^{-2} mol dm^{-3}. Guest only (solid line).

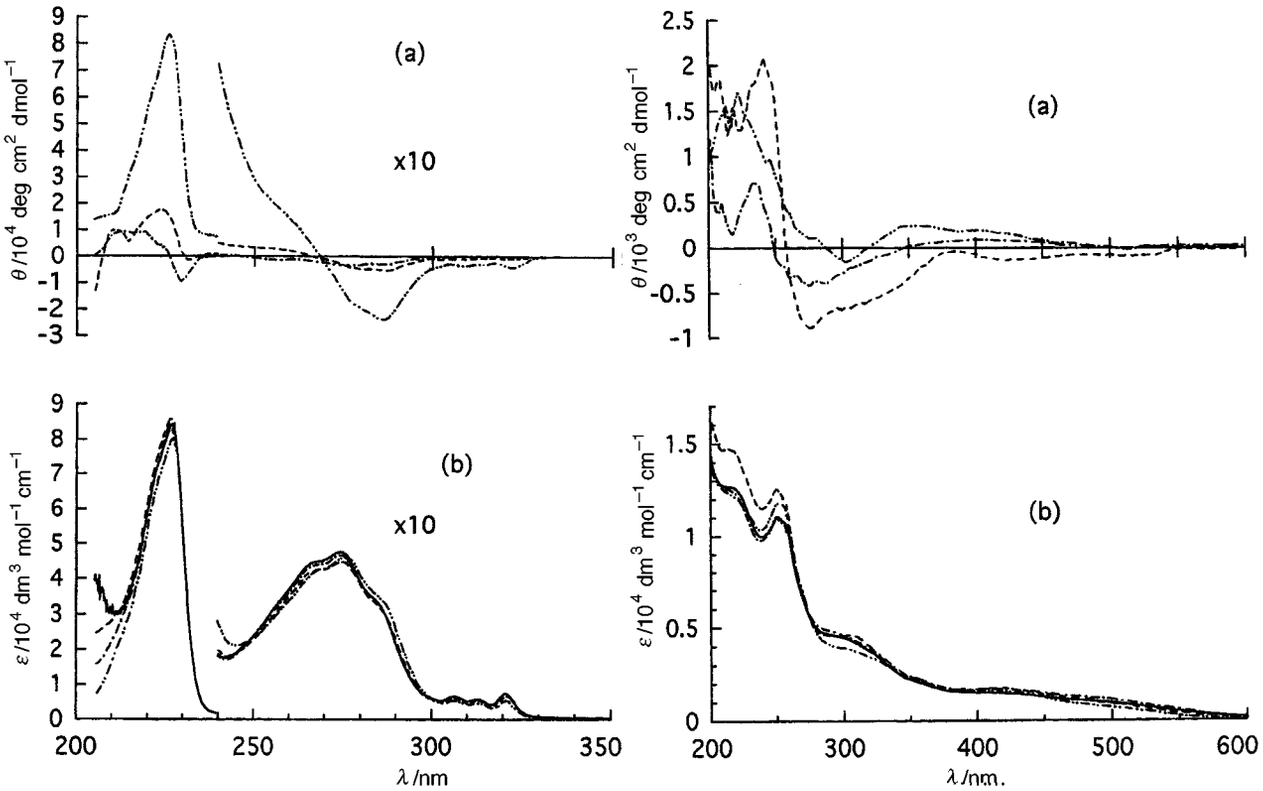

Fig. 9 Induced circular dichroism (a) and absorption (b) spectra of the *α*- (-·-·-), *β*- (-···-···-), and *γ*-cyclodextrin (----) complexes of sodium naphthalenesulfonate (left) and 1-amino-2-naphthol [right; 20%(v/v) ethanol–water] at pH 7 and 25 °C. [cyclodextrins] = 1.2×10^{-2} mol dm^{-3}. Guest only (solid line).

Table 3 Solution species and chirality of the inclusion complexes of **1**–**8**

Compound	*α*-CDx	*β*-CDx	*γ*-CDx
1[a]	1:1	1:1	1:1
2[a]	1:1	2:2 (−)	2:2 (−)
3	1:1	1:1	1:1
4	1:1	1:1	1:1[b]
5	[c]	2:2 (−)	2:2 (−)
6	[c]	2:2 (+)	2:2 (−)
7	[c]	[d]	2:2 (−)
8	1:1	2:2 (−)	[d]

[a] Ref. 2*c*. [b] Probably a 1:1 complex, but a slightly split-type negative ICD spectrum was given. [c] Very weak 1:1 complex. [d] Very obscure split-type ICD spectrum.

with *α*-CDx due to the presence of an *o*-OH group[6] which induces little asymmetry in **6** and **7**. However, in **8** which has no *o*-OH group, a fairly large negative ICD was observed at the π–π* transition of the –N=N– group and the naphthalene moiety (Fig. 7).

This unexpected negative ICD in **8**–*α*CDx would be due to the external association with *α*-CDx in which the –N=N– group is not sufficiently included up to the –N=N– group within the *α*-CDx cavity. A similar reversal of ICD signs has been found in the acridine– and phenazine–*α*CDx complexes[1a] and the heptyl viologen–*α*CDx complex.[15]

Finally, Table 3 shows a summary of the solution species mainly detected by the ICD spectra and chirality of the inclusion complexes of **1**–**8**. The guest molecules with a large bulky hydrophobic substituent or the keto–enol equilibrium tend to form the chiral dimer inclusion complex.

Other cyclodextrin–guest systems

Fig. 8 shows the ICD and absorption spectra of the inclusion complexes of **9** and **10** with *α*-, *β*-, and *γ*-CDx. General ICD patterns of the strong positive ICD at the long-axis polarized π–π* transition of the –N=N– group are observed in **9**–*α*CDx, **9**–*β*CDx, **10**–*α*CDx and **10**–*γ*CDx, indicating the long-axis inclusion of guest into the CDx cavity. In **9**–*γ*CDx which has

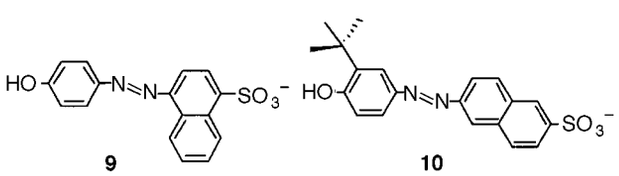

9 **10**

no alkyl substituent, the strong positive ICD shifts to longer wavelength due to the incompatible binding with *γ*-CDx. The unusually small negative ICD of **10**–βCDx at the π–π* band of the –N=N– group has often been observed in *β*-CDx complexes with azo guests having a Bu^t group.[2c]

Attempts to obtain the simple ICD pattern using the naphthalene derivatives

Since the azo guests **3**–**10** have a naphthalene nucleus, it is worthwhile to measure the ICD spectra of some naphthalene derivatives, **11** and **12**, as constituent fragments. There are typically three bands at 300–330(vw), 250–300(w), and 227(s) nm which are attributed to ^1L_b, ^1L_a and ^1B_b transitions of the naphthalene chromophore[16] of **11** and **12**, respectively (Scheme 4).

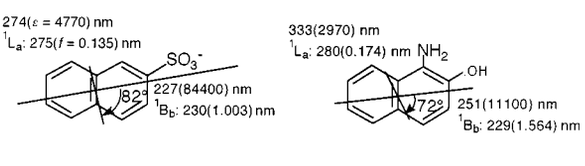

11 **12**

Scheme 4

The ^1L_b and ^1L_a transitions give a small negative ICD, while the ^1B_b transition gives a positive ICD as observed in **11**–*β*CDx and **11**–*γ*CDx (Fig. 9). The strong enhancement in the ICD signal suggests the formation of the more tight complex of **11**–*β*CDx. Therefore, the long-axis polarized ^1B_b transition of **11** is parallel to the molecular axis of the CDx cavity. In **11**–*α*CDx, a somewhat split-type ICD spectrum is observed at the ^1B_b transition band. Similar ICD patterns are also observed in **12**–*α*CDx, **12**–βCDx and **12**–*γ*CDx.

References

1 (*a*) J. M. Schuette, T. T. Ndou and I. M. Warner, *J. Phys. Chem.*, 1992, **96**, 5303; (*b*) H. Yamaguchi and M. Higashi, *J. Inclusion Phenom. Mol. Recognit. Chem.*, 1987, **5**, 725; (*c*) N. Kobayashi, Y. Hino, A. Ueno and T. Osa, *Bull. Chem. Soc. Jpn.*, 1983, **56**, 1849; (*d*) H. Shimizu, A. Kaito and M. Hatano, *J. Am. Chem. Soc.*, 1982, **104**, 7059; (*e*) H. Shimizu, A. Kaito and M. Hatano, *Bull. Chem. Soc. Jpn.*, 1981, **54**, 513; (*f*) H. Yamaguchi and S. Abe, *J. Phys. Chem.*, 1981, **85**, 1640; (*g*) H. Yamaguchi, K. Ninomiya and M. Ogata, *Chem. Phys. Lett.*, 1980, **75**, 593; (*h*) H. Shimizu, A. Kaito and M. Hatano, *Bull. Chem. Soc. Jpn.*, 1979, **52**, 2678; (*i*) H. Yamaguchi, N. Ikeda, F. Hirayama and K. Uekama, *Chem. Phys. Lett.*, 1978, **55**, 75; (*j*) N. Ikeda and H. Yamaguchi, *Chem. Phys. Lett.*, 1978, **56**, 167; (*k*) H. Yamaguchi, N. Ikeda, K. Uekama and F. Hirayama, *Z. Phys. Chem.*, 1978, **109**, 173; (*l*) K. Harata and H. Uedaira, *Bull. Chem. Soc. Jpn.*, 1975, **48**, 375; (*m*) I. Tinoco, Jr., *Adv. Chem. Phys.*, 1962, 4, 113; (*n*) J. P. Kirkwood, *J. Chem. Phys.*, 1937, **5**, 479.

2 (*a*) K. Kano, S. Arimoto and T. Ishimura, *J. Chem. Soc., Perkin Trans. 2*, 1995, 1661; (*b*) S. Tamagaki, K. Fukuda, H. Maeda, N. Miura and W. Tagaki, *J. Chem. Soc., Perkin Trans. 2*, 1995, 389; (*c*) N. Yoshida, H. Yamaguchi and M. Hagashi, *J. Chem. Soc., Perkin Trans. 2*, 1994, 2507; (*d*) K. Kano, K. Yoshiyasu, H. Yoshioka, S. Hata and S. Hashimoto, *J. Chem. Soc., Perkin Trans. 2*, 1992, 1265; (*e*) K. Kano, N. Tsujino and M. Kim, *J. Chem. Soc., Perkin Trans. 2*, 1992, 1747; (*f*) K. Kano, M. Tatsumi and S. Hashimoto, *J. Org. Chem.*, 1991, **56**, 6579; (*g*) M. Suzuki, M. Kajtar, J. Szejtli, M. Vikmon, E. Fenyvesi and L. Szente, *Carbohydr. Res.*, 1991, 214, 25; (*h*) V. Buss, *Angew. Chem., Int. Ed. Engl.*, 1991, **30**, 869; (*i*) R. J. Clarke, J. H. Coates and S. F. Lincoln, *J. Chem. Soc., Faraday Trans. 1*, 1986, **82**, 2333; (*j*) R. J. Clarke, J. H. Coates and S. F. Lincoln, *J. Chem. Soc., Faraday Trans. 1*, 1984, **80**, 3119.

3 H. Shinmori, M. Takeuchi and S. Shinkai, *J. Chem. Soc., Perkin Trans. 2*, 1998, 847; R. Ambrosetti, R. Bianchini, S. Fisichella, M. Fichera and M. Zandomeneghi, *Chem. Eur. J.*, 1996, **2**, 149; X. Song, J. Perlstein and D. G. Whitten, *J. Am. Chem. Soc.*, 1995, **117**, 7816; K. Murata, M. Aoki and S. Shinkai, *Chem. Lett.*, 1992, 739; M. Shimomura, R. Ando and T. Kunitake, *Ber. Bunsenges. Phys. Chem.*, 1983, **87**, 1134; M. Hatano, M. Yoneyama, Y. Sato and Y. Kawamura, *Biopolymers*, 1973, **12**, 2423.

4 U. D. Rossi, S. Dähne, S. C. J. Meskers and H. P. J. M. Dekkers, *Angew. Chem., Int. Ed. Engl.*, 1996, **35**, 760; D. J. Owen and B. Schuster, *J. Am. Chem. Soc.*, 1996, **118**, 259; H. Ihara, M. Shibata and C. Hirayama, *Chem. Lett.*, 1992, 1731.

5 (*a*) N. Yoshida, H. Yamaguchi and M. Higashi, *J. Phys. Chem. A.*, 1998, **102**, 1523; (*b*) N. Yoshida, *J. Chem. Soc., Perkin Trans. 2.*, 1995, 2249; (*c*) N. Yoshida and Y. Fujita, *J. Phys. Chem.*, 1995, **99**, 3671; (*d*) N. Yoshida and K. Hayashi, *J. Chem. Soc., Perkin Trans. 2*, 1994, 1285; (*e*) N. Yoshida and M. Fujimoto, *J. Phys. Chem.*, 1987, **91**, 6691.

6 N. Yoshida, A. Seiyama and M. Fujimoto, *J. Phys. Chem.*, 1990, **94**, 4254.

7 N. Yoshida, A. Seiyama and M. Fujimoto, *J. Phys. Chem.*, 1990, **94**, 4246.

8 S. Anderson, T. D. W. Claridge and H. L. Anderson, *Angew. Chem., Int. Ed. Engl.*, 1997, **36**, 1310; G. R. Hodges, J. R. L. Smith and J. Oakes, *J. Chem. Soc., Perkin Trans. 2*, 1998, 617.

9 J. Ridley and M. C. Zerner, *Theor. Chim. Acta*, 1973, **32**, 111; W. P. Anderson, W. D. Edwards and M. C. Zerner, *Inorg. Chem.*, 1986, **25**, 2728.

10 MOPAC Ver 6: J. J. P. Stewart, *QCPE Bull.*, 1989, **9**, 10. Revised as Ver 6.01 by T. Hirano, University of Tokyo, for the HITAC machine: *JCPE News*, 1991, **2**, 26.

11 *Circular Dichroism—Principle and Applications*, ed. K. Nakanishi, N. Berova and R. W. Woody, 1994, VCH Publishers, Inc; M. Siam, G. Blaha and H. Lehner, *J. Chem. Soc., Perkin Trans. 2*, 1998, 853; S. E. Boiadjiev, D. T. Anstine and D. A. Lightner, *J. Am. Chem. Soc.*, 1995, **117**, 8727; D. Lightner and J.-Y. An, *Tetrahedron*, 1987, **43**, 4287; N. Harada and K. Nakanishi, *Acc. Chem. Res.*, 1972, **5**, 257.

12 N. Yoshida and M. Fujimoto, *Bull. Chem. Soc. Jpn.*, 1979, **52**, 2527.

13 R. L. Reeves and R. S. Kaiser, *J. Org. Chem.*, 1970, **35**, 3670; S. Suzuki, R. C. Das and K. Harada, *Bull. Chem. Soc. Jpn.*, 1978, **51**, 2136; J. E. Kuder, *Tetrahedron*, 1972, **28**, 1973; J. Oakes and P. Gratton, *J. Chem. Soc., Perkin Trans. 2*, 1998, 2201.

14 M. Kasha, H. R. Rawls and M. A. E. Bayoumi, *Pure Appl. Chem.*, 1965, **11**, 371.

15 M. Kodaka, *J. Phys. Chem.*, 1991, **95**, 2110; M. Kodaka and T. Furuya, *Bull. Chem. Soc. Jpn.*, 1989, **62**, 1154.

16 R. S. Becker, *Theory and Interpretation of Fluorescence and Phosphorescence*, 1971, John Wiley & Sons, Inc., New York.

Paper 8/03729I